Energy & Environmental Science

Accepted Manuscript

ROYAL SOCIETY OF CHEMISTRY

www.rsc.org/ees

Energy & Environmental Science

Dynamic Article Links ►

Cite this: DOI: 10.1039/c0xx00000x

ARTICLE TYPE

www.rsc.org/xxxxxx

Efficient Hydrogen Release from Perhydro-N-ethylcarbazole Using Catalyst-Coated Metallic Structures Produced by Selective Electron Beam Melting

W. Peters,[a] M. Eypasch,[b] T. Frank,[b] J. Schwerdtfeger,[c] C. Körner,[c] A. Bösmann,[a] P. Wasserscheid[a]*

Received (in XXX, XXX) Xth XXXXXXXXX 20XX, Accepted Xth XXXXXXXXX 20XX
DOI: 10.1039/b000000x

A particularly suitable reactor concept for the continuous dehydrogenation of perhydro-N-ethylcarbazole in the context of hydrogen and energy storage applications is described. The concept addresses the fact that dehydrogenation is a highly endothermic gas evolution reaction. Thus, for efficient dehydrogenation a significant amount of reaction heat has to be provided to a reactor that is essentially full of gas. This particular challenge is addressed in our study by the use of a catalyst coated (Pt on alumina), structured metal reactor obtained by Selective Electron Beam Melting. The so-obtained reactor was tested both as single tube set-up and as Hydrogen Release Unit (HRU) with ten parallel reactors. The HRU realized in stationary operation a hydrogen release capacity of 1.75 kW_{therm} (960 W_{el} at subsequent fuel cell) with up to 1.12 g_{H2} min^{-1} g_{Pt}^{-1} and a power density of 3.84 kW_{el} $liter^{-1}$ of HRU reactor.

1. Introduction

While today's energy system is largely based on the consumption of fossil fuels there are many good reasons to promote a step-wise transition to electricity production from renewable sources, such as wind and solar power. Important arguments are the limited availability of fossil fuels on the long run and the foreseeable consequences of an anthropogenic climate change.

The key challenge for the massive integration of renewable energy into our energy system is its intermittent character. The production output of e.g. wind turbines and solar PV units is primarily determined by meteorological parameters with strong seasonal, day-time and weather dependent fluctuations. Countries with a large share of wind and solar energy, such as e.g. Germany, already experience the problem of energy over-production on very windy or sunny days while their large wind and sun power installations do hardly contribute to electricity production during unfavorable weather conditions. Consequently, a stable and reliable energy supply by renewable energies requires storage technologies that enable balancing of energy over- and underproductions. A significant part of such future energy storage systems should enable lossless storage of large amounts of energy over long time periods in order to allow seasonal or day-time buffering. Based on today's technologies such task cannot be accomplished reasonably by mechanical and electrochemical methods alone but requires chemical energy storage technologies.

Hydrogen produced by water electrolysis is considered as a suitable energy carrier due to its high gravimetric energy density (120 MJ kg^{-1}). The generation of electricity, heat or mechanical power from hydrogen involves oxidation of the latter in a fuel cell or combustion engine producing water thus closing the material balance of this carbon-free energy storing cycle.

A major drawback of using hydrogen as energy carrier is its low volumetric storage density. At ambient conditions (1 bar, 25°C), one litre of hydrogen contains only 0.003 kWh of thermal energy. Even as compressed gaseous form (CGH2, typically at 700 bar pressure) or as liquefied cryogenic hydrogen (LH2, typically at -253°C) the volumetric storage density of elemental hydrogen is still low, with energy contents of 1.3 and 2.4 kWh L^{-1}, respectively. In addition, H_2 compression and cooling costs some energy and both forms of hydrogen handling require special infrastructure such as compressor stations, pipelines, pressure-resistant containers or cryogenic tank systems. Furthermore, it is difficult to imagine that the handling of large amounts of elemental hydrogen by a broad and untrained public at very high pressures or very low temperatures will work out without applying sophisticated and expensive safety technologies.

A very promising concept that avoids new infrastructure and utilizes existing infrastructure is chemical energy storage, i.e. the

[a] *Department of Chemical and Biological Engineering, University of Erlangen-Nuremberg, Egerlandstr. 3, 91058 Erlangen, Germany.*
[b] *BMW Group Forschung und Technik, Hanauer Straße 46, 80992 München, Germany.*
[c] *Department of Material Science, University of Erlangen-Nuremberg, Martensstrasse 5, 91058 Erlangen, Germany.*
* *Corresponding Author, Tel: +49-9131-8527420, Email: peter.wasserscheid@fau.de*

reversible chemical conversion of hydrogen in the form of hydrogen-rich chemicals. Figure 1 shows the general concept of binding hydrogen from renewable sources to a hydrogen-lean molecule, for the example of the Liquid Organic Hydrogen Carrier (LOHC) system N-ethyl carbazole (NEC) / perhydro-N-ethyl carbazole (H12-NEC).

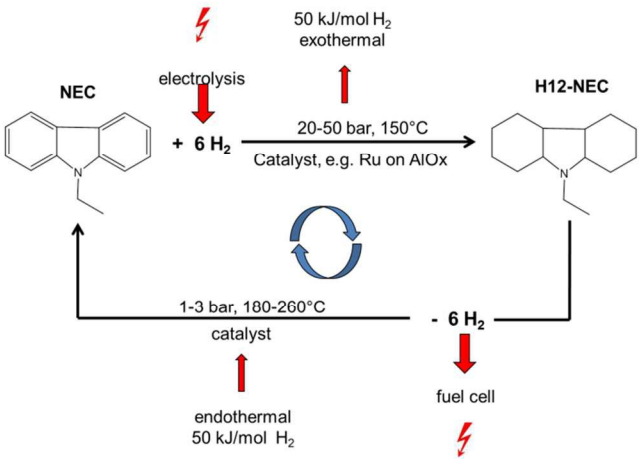

Fig. 1 Storage and transport of renewable energy equivalents in form of hydrogen-rich liquid chemicals based on reversible hydrogenation/dehydrogenation cycles.

The liquid nature of both the hydrogen-rich and the hydrogen-lean form of the hydrogen storage system facilitates storage and transport in the existing infrastructure for liquid fuels. Note that the melting point of pure NEC is 68°C but mixtures with partly dehydrogenated species are liquids at ambient. Moreover, it is particularly interesting to use liquids as hydrogen-lean molecules as this allows for a closed material cycle without binding or releasing other substances from the atmosphere than water and oxygen (in contrast to systems that use e.g. N_2 or CO_2 as hydrogen-lean molecules of the chemical energy storage system). The rationale behind LOHC energy storage systems is that energy is stored during energy-rich times (high solar intensity, strong wind, cheap energy) by LOHC hydrogenation while hydrogen is released at times and places which are energy deficient by catalytic dehydrogenation.[1,2]

The hydrogen storage capacity of the LOHC system NEC/H12-NEC is 5.8 wt% if full dehydrogenation is considered and 5.2 wt% if the reaction should result in a liquid, hydrogen-lean mixture. The exothermal, catalytic hydrogenation of NEC to H12-NEC (upper part of Figure 1) is typically promoted by Ru-catalysts and releases 50 kJ per mol H_2 reaction heat.[3–6] The endothermic dehydrogenation (lower part of Figure 1) requires for thermodynamic reasons the same amount of heat at a higher level of reaction temperature.[7,8]

In this contribution we focus on a novel reactor concept to release hydrogen from H12-NEC in a most efficient and productive way. Before going into the details of our study we will summarize shortly the state-of-the-art knowledge with respect to this particular reaction.

A number of studies have been carried out in the recent decade demonstrating that H12-NEC can be dehydrogenated using Pt and Pd based catalysts.[9–12] Alumina, silica and carbon have been used as porous supports.[6,11,13] So far, kinetic studies have been mostly restricted to batch experiments.[5,8,10,13–15] In these studies it has been found that the reaction from H12-NEC to NEC proceeds stepwise over the main intermediates H8-NEC and H4-NEC.[16,17] The activation energy of the dehydrogenation reaction has been reported to be in the range of 118-127 kJ mol_{H2}^{-1}.[16] Detailed mechanistic insight on the dehydrogenation reaction of H12-NEC has been recently gained by surface science studies on different Pd and Pt model catalysts.[11,12,18,19]

2. Dehydrogenation reactor concepts

From a reaction engineering point of view the dehydrogenation of H_2-rich LOHCs is complicated by the very large volume of hydrogen gas generated in the reactor (> 650 mL H_2 per mL H12-NEC converted to H0-NEC) and by the need to transport the significant reaction heat to the catalytic sites. In this context, Wild *et al.* and Toseland *et al.* suggested a microwick reactor and a micro tube[5,18] while Cooper *et al.* proposed the application of a micro reactor.[9,20,21] For easy removal of the product gas from the catalytic surface Hodoshima *et al.* and Karyia *et al.* reported a concept where the dehydrogenation catalyst is covered with a thin liquid LOHC film or is applied under dynamic wet/dry conditions.[22,23] Later the group of Kariya applied a spray-pulse reactor for LOHC dehydrogenation.[24] Hydrogen evolution rates of up to 7.6 g H_2 per g catalyst and min were reported with such devices in the cyclohexane dehydrogenation at 350°C using a Pt/Al_2O_3 catalyst.[25,26] Recently, Shukla *et al.* reviewed the different tested reactor concepts for LOHC dehydrogenation and stated correctly that there is only little information available on the application of monolithic reactors which, nevertheless, are characterized with a number of very attractive features for this hydrogen release reaction.[27] In general, structured reactors, such as monolithic or foam reactors, exhibit the important advantage over catalytic fixed beds that their structure provides high heat conductivity and thus allows good heat input for endothermic reactions.[28–33] The range of applicable structured reactors, both with respect to the material (e.g. SiC, Cu, aluminium, aluminium oxide) and the structure (e.g. mesh structures, foams, honeycombs) is huge and this variability is often considered as a great advantage.[34–36] The high porosity of some monoliths provides a very low pressure drop which is very important for reactions with significant volume expansion, such as e.g. the dehydrogenation of hydrogen-rich LOHCs.[37,38]

A novel concept for the manufacturing of structured metallic reactor systems is the use of additive manufacturing (AM), especially in the form of powder bed based processes like selective electron beam melting (SEBM).[39–42] In this manufacturing process the structured reactor is built up layer-by-layer. The reactor wall and the inner 3D-structure (monolithic, foam like or cellular) are processed simultaneously, resulting in an interconnected reactor structure. Furthermore, it is possible to determine orientation, geometry and size of every strut of a cellular structure. The control over geometric properties translates into control over the physical properties (e.g. mechanical, flow or heat conductivity properties).[37,43–45]

SEBM is a relatively new technology that utilizes an electron beam for the local melting of the metal powder in the powder

bed. This has a number of potential advantages over laser based technologies. As beam control does not rely on mirrors and lenses, but electro-magnetic fields, very high deflection speeds can be realized. In principle any electrically conductive powder can be used as building material for the SEBM process, however, the process is most mature for titanium alloys and specifically Ti-6Al-4V.

Using structured reactors, such as monoliths, foams or cellular structures for catalysis involves in most cases the coating of a catalytic active layer onto the reactor through deposition processes like chemical vapour deposition,[46–48] atomic or electrophoretic particle deposition,[49,50] spray- [51–54] or dipcoating.[55–57] Typical thicknesses of catalytic active layers on monoliths range from a few microns up to 500 µm.[51,58] In dip- or spray-coating processes a dispersion or a suspension of ceramic or carbon powder is used in the coating process.[28,29,57] Many publications apply coatings of ceramic films using the gel-dipping process.[55,59] Schwieger *et al.* used a low pressure spray coating technique resulting in very adhesive and homogeneous coatings.[53] Extensive work on the coating of different monoliths with different ceramic coatings was reported by Groppi *et al.*.[60–63]

This contribution reports on the development of a hot gas-heated dehydrogenation unit for H12-NEC with a capacity of ca. 1 kW_{el} at a subsequent fuel cell (ca. 2 kW_{therm} with respect to the lower heating value of H_2). By the use of catalytic coated structured metal reactors based on SEBM-manufactured structures the volumetric hydrogen production rate and thus the volumetric power output are optimized.

3. Experimental

SEBM reactor tube manufacturing

The reactor tubes were produced using an Arcam S12 system (Arcam AB, Sweden). The system essentially consists of a control unit, a high voltage unit, the electron beam column and a vacuum chamber in which the actual structure building takes place. We applied in the SEBM process gas atomized Ti-6Al-4V powder with particle size of 45 µm – 105 µm. In order to improve process stability, protective gas at low pressure (He-atmosphere, $2*10^{-3}$ mbar) was used during building. For every layer the process consists of four distinct steps: 1) Powder is spread out in the building area by a rake system in layers of about 100 µm thickness; 2) The powder is preheated using a defocused electron beam to slightly sinter the powder for electrical conductivity and a certain mechanical stability; 3) The powder is locally molten by a focused e-beam according to the desired part geometry; 4) The building platform is lowered by one layer thickness and the process is repeated until the part is finished. When the total building process is completed, the obtained part is surrounded by a shell of sintered metal powder, which has to be removed by "sand" blasting with the same metal powder as used in the building process to ensure recyclability of the powder.

For the Ti-6Al-4V monoliths produced in this work the building temperature was 550 - 600°C. The energy supplied to the powder during the preheating step was lowered to strongly reduce sintering of the metal powder during the process. This bears the danger of destabilizing the process through insufficient charge transport away from the building area which can lead to charging of the metallic powder. However, the lower temperature was necessary as initial trials showed that otherwise the sintered powder could not be removed completely from the inside of the reactor tubes. The complete powder removal was further assisted by introducing a 6 mm channel in the center of the cellular structure and by the large inlet and outlet diameters of the reactor tube.

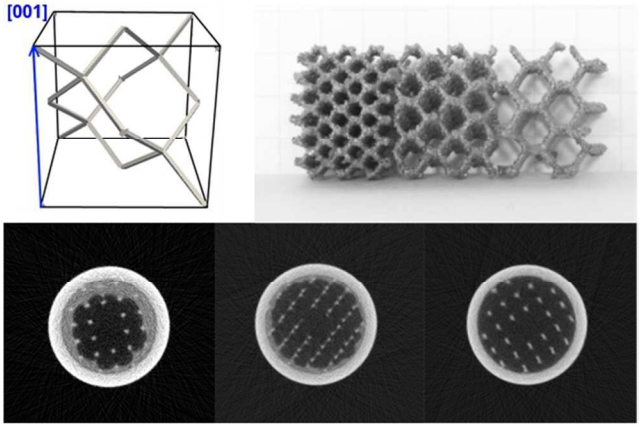

Fig. 2 Top left: Subunit cubic diamond crystal structure; Top right: Different diamond cell sizes manufactured via SEBM-process; Bottom: Powder removal at three different stages, measured via computational tomography at the cross section of a single reactor.

The need for powder removal also defines the lower limit of possible cell sizes in the cellular structure. Figure 2 shows a graduated SEBM structure for optimized gas removal from the reactor as well as three cross sections of the reactor by x-ray tomography to document different stages of powder removal from the reactor.

For our study a cellular structure based on the cubic diamond geometry was chosen.[48,64] The unit cell is shown in Figure 2. The cell size was chosen to be 4.95 mm for the final reactors and the structure was oriented with the [100] direction pointing in the flow direction. Deflection speeds for the beam during melting were in the range of 10^2 mm/s and of 10^4 mm/s during preheating. The cellular structure was built with a beam current at 2 mA and a residence time on each spot of about 3.5 ms. This ensured thin struts in the range of 0.5 mm diameter.

SEBM reactor machining and coating

After removal of metal powder from the reactor the tube surface was trimmed by machining prior to the application of screw threads and sealing surfaces. Aluminium and copper sealings have been applied to verify the pressure tightness. The pressure test was performed at about 55 bar, and the pressure loss was found to be less than 1.5 bar h^{-1}. For coating with the catalytic active layer, a commercial boehmit powder, Disperal (Z500100E, Sasol Germany GmbH) was dispersed in diluted nitric acid solution at a pH of 2. After stirring for about 1h at ambient temperature, a commercial catalyst powder (5% Pt/Alumina, Sigma Aldrich 205974/MKBH3784) was added.

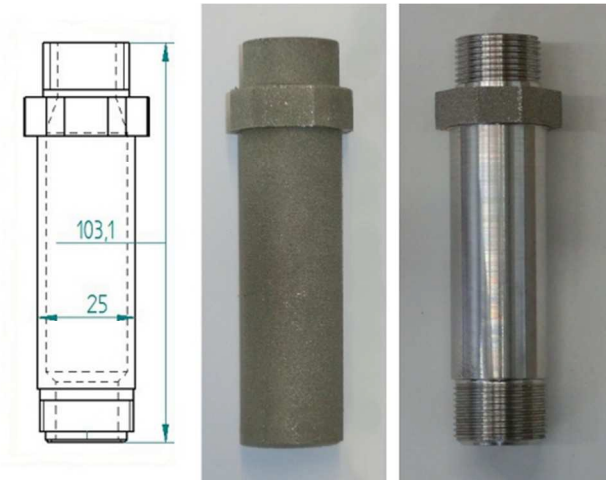

Fig. 3 Single reactor tube manufacturing; Left: Blueprint; Center: Unmachined reactor tube after the SEBM process; Right: Machined reactor: Screw threads and sealing surfaces manufacturing using conventional methods.

The obtained suspension containing 7.5 wt. % of AlO(OH) and 7.5 wt.% catalyst powder was stirred for another hour. The coating was performed by filling the reactor tube with the suspension, which remained inside the reactor for about 30 s. Since the effect of the withdrawal velocity on the coating thickness is well known, a low percolation velocity was chosen.[55] Subsequent to the coating, the reactor was dried in a ventilated oven at 280°C for 15 minutes. For higher coating thicknesses the procedure was repeated. The reactor was calcined in air at 500°C for 6 h to stabilize the coating. The finally coated mass was 3.5 g per reactor. Thus, coating thicknesses of more than 150 microns were realized.

Single dehydrogenation test reactor

The dehydrogenation of H12-NEC was conducted in a single reactor tube. The reactor tube was mounted in a ventilated oven (Figure 4). The reactions were carried out under continuous H12-NEC flow using a HPLC pump with flow rates ranging from 0.5-4 mL min^{-1} at temperatures between 220°C and 260°C and at ambient pressures. H12-NEC was purchased from Hydrogenious Technologies GmbH (www.hydrogenious.net).

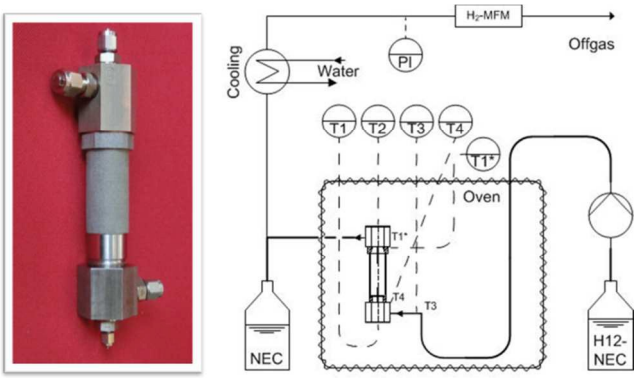

Fig. 4 Set-up for catalytic tests of a single SEBM reactor; Left: Single reactor tube with fittings at reactor head and bottom after machining; Right: Single reactor tube test setup in a heated oven with multiple temperature measurement and H_2-flow rate detection via a hydrogen mass flow meter.

Hydrogen Release Unit (HRU) consisting of ten parallel reactors and test set-up

Furthermore, a tenfold, parallel reactor setup has been developed to realize higher hydrogen evolution in a multi-reactor set-up. To demonstrate heat integration with a high temperature hydrogen combustion unit (e.g. a hydrogen burner or a solid oxide fuel cell), the HRU was designed for hot air heating (up to 450°C; 200 NL min^{-1} volumetric flow). Technical details of the applied test set-up are given as Supporting Information. The total volume of the applied HRU (Figure 5) is 4 liter while the total reactor volume of the ten reactors is only 250 mL. The pre-heated H12-NEC is fed into the ten reactors through the unit bottom. The dehydrogenated products as well as the released hydrogen leave the reactor at the top where in the reactor head gas/liquid separation takes place. Subsequently, the hydrogen flow rate is measured via a hydrogen mass flow meter and the H_2 is fed into a fuel cell for electricity production.

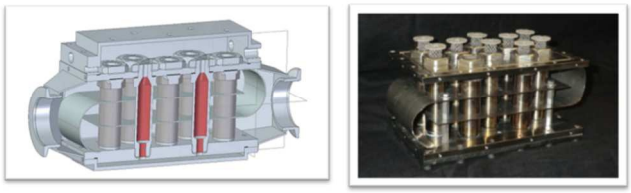

Fig. 5 Hydrogen release unit (HRU) consisting of ten parallel reactors mounted in vertical direction. Left: Schematic view showing the reactors in the hot air box – hot air enters the box from the left to ensure counter-current heat transfer; Right: Photograph of the open HRU unit with ten SEBM-manufactured and catalytically functionalized reactor tubes. The unit is surrounded by a box to guide the hot air flow.

Inlet and exit temperatures of the hot air flow are monitored and controlled as well as its volumetric flow rate. Other important parameters that are monitored and controlled in the experiment are the inlet and outlet temperatures of the LOHC flow at the HRU, the reaction temperature inside the reactor tubes (six different measurement points in six different reactor tubes), the hydrogen exit flow and the system pressure. The system pressure of the whole test-rig is 1.6 bar absolute pressure in all experiments reported here. By adjusting the hot air temperature and the volumetric flow rate, we measured three different isotherms of 230, 250 and 260°C for variable H12-NEC flow rates between 10 and 40 mL min^{-1}. The goal is to monitor hydrogen production rates and catalyst productivities under different reaction conditions to identify suitable operation points of the HRU.

4. Results and Discussion

Single reactor tube H12-NEC dehydrogenation results

Single reactor tube experiments have been performed at three different temperatures with varying H12-NEC flow rates. The resulting hydrogen flow rates and the calculated hydrogen yields (amount of hydrogen released/total releasable hydrogen in the LOHC system) are presented in Figure 7.

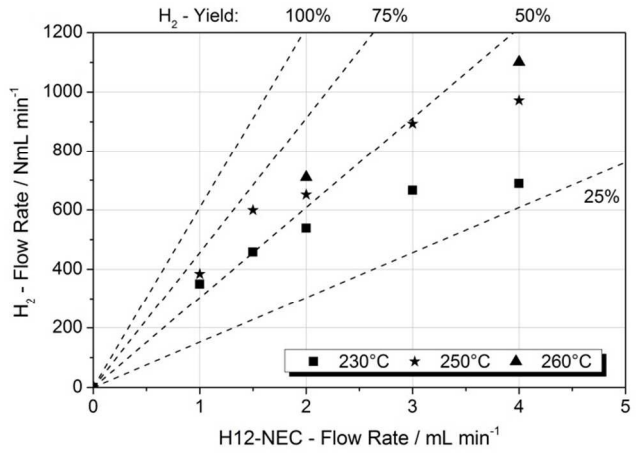

Fig. 7 Hydrogen release rates and hydrogen yields as a function of reaction temperature and H12-NEC flow rates obtained from single reactor tube experiments.

As expected, the reaction rate is higher at higher temperature which is both due to a higher driving force for the endothermic reversible dehydrogenation reaction and due to the higher reaction rate constant at higher temperature. From a kinetic perspective the first hydrogenation step, from H12-NEC to H8-NEC, is known to proceed easiest, while the further dehydrogenation steps to NEC proceed slower.

Table 1 summarizes the single tube results with respect to temperature and hydrogen flow rate deviation. Due to the good heat transfer of the lab setup the temperature deviation remained below 3%. A minor issue was the observed hydrogen flow rate fluctuation of up to 5.4 % within a stationary measurement. Nevertheless a high catalyst activity of 1.27 g_{H2} min^{-1} g_{Pt}^{-1} (260°C, H12-NEC flow rate: 4 mL min^{-1}) could be reached. Considering the volume of the platinum coated reactor as reference, a volumetric activity of 4.32 kW_{el} per liter was achieved.

Table 1 Experimental data of continuous H12-NEC dehydrogenation experiments in a single tube SEBM reactor.

Temperature Nominal °C	Temperature Deviation %	LOHC Flow mL min^{-1}	Hydrogen Yield %	Hydrogen Deviation %	Catalyst Productivity g_{H2} min^{-1} g_{Pt}^{-1}
230	0.7	1.0	57.6	1.4	0.40
	0.9	1.5	50.2	1.6	0.53
	0.7	2.0	39.7	1.5	0.62
	1.1	3.0	36.5	0.6	0.77
	0.6	4.0	28.3	0.8	0.79
250	0.5	1.0	63.2	4.5	0.44
	1.1	1.5	65.7	5.4	0.69
	0.9	2.0	53.5	2.6	0.75
	1.8	3.0	49.0	2.4	1.03
	1.4	4.0	40.0	3.2	1.12
260	1.2	2.0	57.6	4.2	0.82
	2.4	4.0	45.3	3.1	1.27

HRU H12-NEC dehydrogenation results

Applying the HRU (ten parallel reactors) for H12-NEC dehydrogenation it has been found that it takes about 45 minutes to reach steady state in the whole set-up. After that time, however, stationarity was excellent. Figure 8 shows the four main variables of the experiment, namely system pressure, LOHC-inlet temperature, reaction temperature and hydrogen flow rate exemplified for the time interval between 67.5 and 76 min time-on-stream.

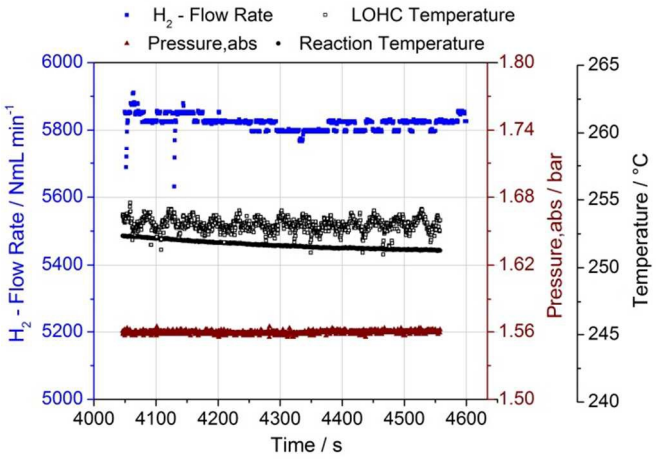

Fig. 8 Steady-state operation of the HRU after a start-up time of 45 min. Conditions: reaction temperature: 230°C; H12-NEC flow rate: 1 mL min^{-1}.

Pressure deviations over this time range were less than 0.05 bar (3 %). Deviation of the LOHC-inlet and reaction temperatures were less than 2°C (1 %), while deviations in hydrogen release were less than 100 mL H_2/min (1.5 %). The spread in temperature of the six different measuring points in 6 different reactors was within 10°C (4 %). Therefore in total we can assume that the experiments in the HRU were operated under steady state with only minor fluctuations.

Table 2 shows the results of a LOHC-flow rate variation at 230, 250 and 260°C. From the obtained data we calculated standard deviations for temperature, pressure and hydrogen yield. Deviation within an experiment, as depicted in Fig. 8, is referred to as stationary, whereas the deviation comparing all experiments is labelled reproduction. Deviation calculations are based on at least 1000 measured values or a period of 10 min to 50 min. The standard deviation of the catalyst productivity is equivalent to the one of the hydrogen yield. The indicated hydrogen yield is the fraction of the released hydrogen over the overall stored hydrogen in the LOHC.

Due to crystallization of NEC (m.p. of pure NEC is 68°C) at very high hydrogen yields, the system pressure rose up to 3.4 bar for some operation points (indicated with "*" in Table 2). This results in a relatively high pressure deviation of up to 41 %. However, as shown in Table 2, there is a rather marginal effect of this pressure fluctuation on the hydrogen yield (as equilibrium is far away) and therefore on the catalyst productivity. The average standard deviation of the hydrogen yield of all measurements is 6.9%, the maximum is 18.2%. This discrepancy results in particular from the use of different batches of H12-NEC with slightly different levels of impurities, such as e.g. H12-carbazole.

Table 2 Continuous H12-NEC dehydrogenation experiments in the HRU. Temperature, pressure and hydrogen flow rate deviations refer to data of reproduction experiments. Stationarity deviation refers to deviation within a stationary operation point; values indivated with "*"were obtained in experiments in which the pressure rose to higher values due to NEC crystallization.

Temperature			LOHC	Pressure		Hydrogen		H_2-Deviation		Catalyst
Nominal	Actual	Deviation	Flow Rate	Actual	Deviation	Flow Rate	Yield	Stationarity	Reproduction	Productivity
°C	°C	°C		bar	%	NmL min^{-1}	%	%	%	g_{H2} min^{-1} g_{Pt}^{-1}
230	230	0.3	10	1.60	0.0	2918	48.2	6.8	6.6	0.33
	231	0.3	20	1.60	3.6	5700	47.1	1.4	1.2	0.65
	229	0.9	30	1.70	4.1	8712	48.0	2.1	12.3	0.99
	230	0.7	40	2.40*	36.9	9313	38.5	0.8	9.0	1.06
250	251	0.6	10	1.60	0.9	4757	78.7	3.7	1.3	0.54
	253	1.0	15	2.80*	33.7	5271	58.1	1.1	8.0	0.60
	247	1.0	20	2.10*	40.8	7100	58.7	1.4	18.2	0.81
	247	0.4	30	1.70	9.8	9789	54.0	2.3	6.1	1.12
260	260	0.3	10	2.60*	5.7	4762	78.7	-	0.8	0.54
	261	0.3	15	1.67	5.7	6609	72.9	1.4	5.5	0.75

From the data in Table 2 the thermal and potential electric power of the HRU under investigation can be determined according to equation 1.

$$P_{therm} = \rho * V_{H2} * LHV_{H2} \quad (1)$$

Calculating with the Lower Heat Value (LHV) of hydrogen of 120 MJ kg^{-1} and the volumetric density (ρ) of hydrogen of 0.0899 kg m^{-3} at standard conditions, the flow rate of 9.8 NL min^{-1} (as obtained in the HRU experiments at 250°C, see Table 2) results in 1.75 kW thermal power or 960 W electric power (using a fuel cell with 55 % efficiency). The results listed in Table 2 are further illustrated in Figure 9 where the hydrogen flow rates and the hydrogen yields of the HRU are plotted over the LOHC flow rate.

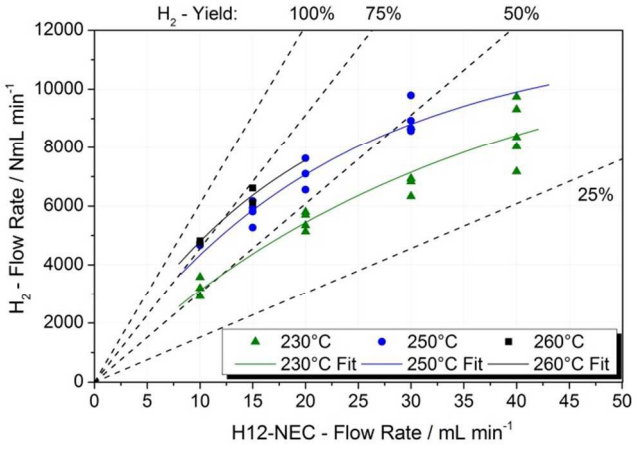

Fig. 9 Hydrogen release rates and hydrogen yields as a function of reaction temperature and H12-NEC flow rate as obtained in H12-NEC dehydrogenation experiments using the HRU; depicted fits do not represent kinetic models but aim to illustrate general tendencies based on the average H_2-flow rate values at each temperature and H_{12}-NEC flow rate.

As expected, H_2 yields go down with increasing LOHC flow rates due to lower residence times in the reactor, while catalyst productivity rises due to fast dehydrogenation of H12-NEC to H8-NEC. For high H12-NEC flow rates productivities of up to 1.12 g_{H2} min^{-1} g_{Pt}^{-1} are obtained.

To check catalyst stability, system control and reproducibility, several operation points of the HRU were adjusted at the beginning of a 48-hour continuous dehydrogenation experiment (within the first 10 hours) and at the end of the run (within the last 10 hours). Fig. 10 gives H_2-flow rate and productivity data for this type of stability test under continuous operating conditions for 48 hours time-on-stream.

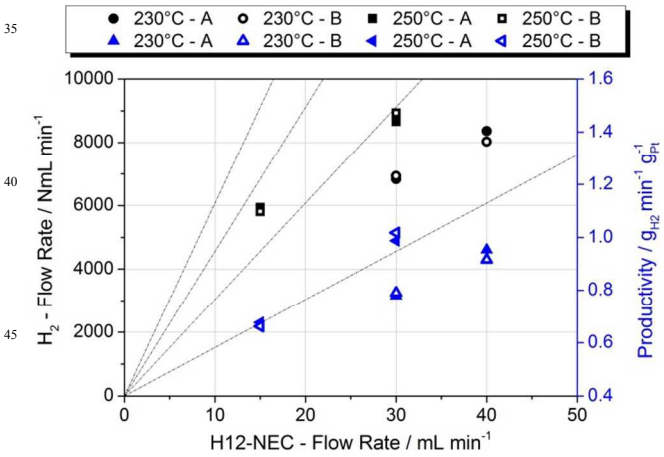

Fig. 10 System stability for continuous H12-NEC dehydrogenation using the HRU within 48 hours time-on-stream. (A): First results (within first 10 hours of experiment) – (B) reproduction (within last 10 hours of the experiment).

In general, system stability and reproducibility is very high. The average standard deviation of hydrogen yield is only 1.9 % and corresponds to small discrepancies in reaction temperature and pressure of 1 % and 3.9 %, respectively. Thus we conclude that continuous operation of the here presented HRU is possible in a quasi-stationary manner over at least 48 hours time-on-stream.

Due to practical limitations of our test rig it was not possible to further increase hydrogen yield or catalyst productivity. Main limitations were the operation range of the LOHC pump and the performance of the applied hot air gun. To avoid inhomogeneous heat input we restricted LOHC flow rates to 30 mL min^{-1} at 250°C and even to 15 mL min^{-1} at 260°C.

5. Conclusions and outlook

The conversion of our current carbon-based energy system to a hydrogen-based one requires effective ways to store hydrogen in large amounts over long periods of time. LOHCs have the potential to substitute step-by-step liquid fossil fuels as they are energy carriers with attractive energy density and diesel-like handling. Hydrogen release from H_2-rich LOHC systems allows the on-demand utilization of regenerative energy equivalents at any time and at any place if the charging of the LOHC system was carried out with hydrogen from electrolysis of excess regenerative electricity.

In this contribution we have demonstrated that 3-D-structured metallic reactors produced via Selective Electron Beam Melting form very suitable dehydrogenation reactors for perhydro-N-ethylcarbazole after appropriate coating with an active layer of Pt on alumina. Tubular SEBM reactors were successfully manufactured with an interconnected 3-D structured cellular network inside the reactor. The optimization of the foam network structure towards optimal heat conductivity and efficient hydrogen gas removal from the catalytic surfaces has been previously published by our collaboration partners in detail elsewhere.[65]

The prepared catalytic SEBM reactor tubes have been tested in continuous dehydrogenation reactions in a single reactor and in a Hydrogen Release Unit (HRU) consisting of ten identical reactors. Summarizing the HRU hydrogen release experiments, we demonstrated a hydrogen generation of 9.8 NL_{H2} min^{-1} in a total catalytic reactor volume of 250 mL (250°C, 30 mL min^{-1} flow rate of H12-NEC). The corresponding thermal capacity was 1.75 kW which transforms to an electric capacity of 960 W using a fuel cell with 55 % efficiency. The single reactor tube experiments demonstrated a power density of up to 4.32 kW_{el} L^{-1}. In the HRU with its ten parallel reactors this value reduced slightly to 3.84 kW_{el} L^{-1} which is still quite remarkable and promising in the context of future energy storage systems. Based on the total volume of the HRU (including hot gas channels and housing) the realised power density was 0.4 kW $L_{total\ volume}^{-1}$. The developed HRU set-up showed very stable operation after a start-up phase of 45 min. System stability and reproducibility of the dehydrogenation results proved to be excellent within 48 h time-on-stream.

Optimization potential in the here presented hydrogen release system and apparatus is obvious. First, the problems of NEC solidification at very high hydrogen release can be circumvented with more recent LOHC systems that are liquids at room temperature in all hydrogen loading states.[4] Second, a more homogeneous temperature distribution in the tubes has to be realized at high temperatures and high LOHC flow rates. In this study inhomogeneous temperature distribution prevented experiments under the most productive dehydrogenation conditions. We anticipate that an HRU device of the same dimensions could easily exceed power outputs of 5 kW_{el} L^{-1} if proper heat transfer (e.g. by heat transfer oil instead of hot air) allows to maintain 260°C in the reactor with an H12-NEC flow rate of 40 mL min^{-1}. This is a volumetric power density that would make such HRUs highly attractive in the context of zero-emission range extender concepts for mobile applications.

Acknowledgement

The authors acknowledge financial support by the Deutsche Forschungsgemeinschaft (DFG) within the Excellence Cluster "Engineering of Advanced Materials" in the framework of the excellence initiative. The present work was supported by BMW Forschung und Technik GmbH. We thank Christian Schmidt, Michael Zenner, Marco Di-Pierro and Daniel Teichmann for helpful discussions and technical input. The following contributions by members of the Department of Chemical and Biological Engineering of University of Erlangen-Nuremberg, are gratefully acknowledged: Irma Schmidt for the CT-measurements; Tobias Horneber, Cornelia Rauh and Antonia Delgado for fruitful discussions about heat transfer and fluid dynamics; Florian Enzenberger and Wilhelm Schwieger for their support with regard to SEBM structure design and catalytic functionalization.

References

1. M. Klell, H. Eichlseder and M. Sartory, *International Journal of Hydrogen Energy*, 2012, **37**, 11531-11540
2. D. Teichmann, W. Arlt, P. Wasserscheid and R. Freymann, *Energy Environ. Sci.*, 2011, **4**, 2767-2773
3. M. Yang, Y. Dong and H. S. Cheng, *Advanced Materials Research*, 2014, **953-954**, 981-984
4. X. Ye, Y. An and G. Xu, *Journal of Alloys and Compounds*, 2011, **509**, 152-156
5. F. Sotoodeh and K. J. Smith, *Ind. Eng. Chem. Res.*, 2010, **49**, 1018-1026
6. K. M. Eblagon, D. Rentsch, O. Friedrichs, A. Remhof, A. Zuettel, A. J. Ramirez-Cuesta and S. C. Tsang, *International Journal of Hydrogen Energy*, 2010, **35**, 11609-11621
7. D. Teichmann, K. Stark, K. Müller, G. Zöttl, P. Wasserscheid and W. Arlt, *Energy Environ. Sci.*, 2012, **5**, 9044-9054
8. N. Brückner, K. Obesser, A. Bösmann, D. Teichmann, W. Arlt, J. Dungs and P. Wasserscheid, *ChemSusChem*, 2014, **7**, 229-235
9. A. Bernard Toseland, 2009, *DOE Hydrogen Programm*
10. F. Sotoodeh, B. J. Huber and K. J. Smith, *International Journal of Hydrogen Energy*, 2012, **37**, 2715-2722
11. M. Sobota, I. Nikiforidis, M. Amende, B. S. Zanón, T. Staudt, O. Höfert, Y. Lykhach, C. Papp, W. Hieringer, M. Laurin, D. Assenbaum, P. Wasserscheid, H.-P. Steinrück, A. Görling and J. Libuda, *Chem. Eur. J.*, 2011, **17**, 11542-11552
12. M. Amende, S. Schernich, M. Sobota, I. Nikiforidis, W. Hieringer, D. Assenbaum, C. Gleichweit, H.-J. Drescher, C. Papp, H.-P. Steinrück, A. Görling, P. Wasserscheid, M. Laurin and J. Libuda, *Chem. Eur. J.*, 2013, **19**, 10854-10865
13. F. Sotoodeh and K. J. Smith, *J. Phys. Chem. C*, 2013, **117**, 194-204
14. F. Sotoodeh and K. J. Smith, *Journal of Catalysis*, 2011, **279**, 36-47
15. F. Sotoodeh, B. J. Huber and K. J. Smith, *Applied Catalysis A: General*, 2012, **419**, 67-72
16. F. Sotoodeh, L. Zhao and K. J. Smith, *Applied Catalysis A: General*, 2009, **362**, 155-162
17. M. Yang, C. Han, G. Ni, J. Wu and H. Cheng, *International Journal of Hydrogen Energy*, 2012, **37**, 12839-12845
18. M. Amende, C. Gleichweit, K. Werner, S. Schernich, W. Zhao, Lorenz, Michael P. A., O. Höfert, C. Papp, M. Koch, P. Wasserscheid, M. Laurin, H.-P. Steinrück and J. Libuda, *ACS Catal.*, 2014, **4**, 657-665
19. M. Amende, C. Gleichweit, S. Schernich, O. Höfert, Lorenz, Michael P. A., W. Zhao, M. Koch, K. Obesser, C. Papp, P. Wasserscheid, H.-P. Steinrück and J. Libuda, *J. Phys. Chem. Lett.*, 2014, **5**, 1498-1504
20. G. Pez and B. Toseland, *Air Products Presentation*,2005

21. J. von Wild, T. Friedrich, A. Cooper, B. Toseland, G. Muraro, W. TeGrotenhuis, Y. Wang, P. Humble and A. Karim, *Proceedings of the WEHC,*2010
22. S. Hodoshima, H. Arai and Y. Saito, *International Journal of Hydrogen Energy*, 2003, **28**, 197-204
23. N. Kariya, A. Fukuoka and M. Ichikawa, *Applied Catalysis A: General*, 2002, **233**, 91-102
24. N. Kariya, A. Fukuoka, T. Utagawa, M. Sakuramoto, Y. Goto and M. Ichikawa, *Applied Catalysis A: General*, 2003, **247**, 247-259
25. R. B. Biniwale and M. Ichikawa, *Chemical Engineering Science*, 2007, **62**, 7370-7377
26. R. B. Biniwale, N. Kariya and M. Ichikawa, *Catal Lett*, 2005, **105**, 83-87
27. J. V. Pande, A. Shukla and R. B. Biniwale, *International Journal of Hydrogen Energy*, 2012, **37**, 6756-6763
28. Y. Peng, *Applied Catalysis A: General*, 2004, **266**, 235-244
29. J. Richardson, Y. Peng and D. Remue, *Applied Catalysis A: General*, 2000, **204**, 19-32
30. L. Giani, G. Groppi and E. Tronconi, *Ind. Eng. Chem. Res*, 2005, **44**, 9078-9085
31. L. Giani, G. Groppi and E. Tronconi, *Ind. Eng. Chem. Res*, 2005, **44**, 4993-5002
32. G. Groppi, L. Giani and E. Tronconi, *Ind. Eng. Chem. Res*, 2007, **46**, 3955-3958
33. E. Tronconi and G. Groppi, *Chemical Engineering Science*, 2000, **55**, 6021-6036
34. F. Kapteijn, T. Nijhuis, J. Heiszwolf and J. Moulijn, *Catalysis Today*, 2001, **66**, 133-144
35. M. T. Kreutzer, F. Kapteijn and J. A. Moulijn, *Catalysis Today*, 2006, **111**, 111-118
36. T. J. Schildhauer, K. Pangarkar, van Ommen, J. Ruud, J. Nijenhuis, J. A. Moulijn and F. Kapteijn, *Chemical Engineering Journal*, 2012, **185**, 250-266
37. A. Inayat, J. Schwerdtfeger, H. Freund, C. Körner, R. F. Singer and W. Schwieger, *Chemical Engineering Science*, 2011, **66**, 2758-2763
38. A. Pestryakov, E. Yurchenko and A. Feofilov, *Catalysis Today*, 1996, **29**, 67-70
39. J. Bauer, S. Hengsbach, I. Tesari, R. Schwaiger and O. Kraft, *Proceedings of the National Academy of Sciences*, 2014, **111**, 2453-2458
40. J. Schwerdtfeger, P. Heinl, R. F. Singer and C. Körner, *Phys. Status Solidi (b)*, 2010, **247**, 269-272
41. J. Schwerdtfeger, F. Wein, G. Leugering, R. F. Singer, C. Körner, M. Stingl and F. Schury, *Adv. Mater.*, 2011, **23**, 2650-2654
42. J. Wieding, A. Jonitz and R. Bader, *Materials*, 2012, **5**, 1336-1347
43. A. Inayat, H. Freund, T. Zeiser and W. Schwieger, *Chemical Engineering Science*, 2011, **66**, 1179-1188
44. J. Schwerdtfeger, F. Schury, M. Stingl, F. Wein, R. F. Singer and C. Körner, *Phys. Status Solidi B*, 2012, **249**, 1347-1352
45. M. Klumpp, A. Inayat, J. Schwerdtfeger, C. Körner, R. F. Singer, H. Freund and W. Schwieger, *Chemical Engineering Journal*, 2014, **242**, 364-378
46. R. Ali, E. Alkhateeb, F. Kellner, S. Virtanen and N. Popovska-Leipertz, *Surface and Coatings Technology*, 2011, **205**, 5454-5463
47. G. Emig, N. Popovska and G. Schoch, *Thin Solid Films*, 1994, **241**, 361-365
48. T. Knorr, P. Heinl, J. Schwerdtfeger, C. Körner, R. F. Singer and B. J. Etzold, *Chemical Engineering Journal*, 2012, **181-182**, 725-733
49. P. Rodriguez, B. Caussat, X. Iltis, C. Ablitzer and M. Brothier, *Chemical Engineering Journal*, 2012, **211-212**, 68-76
50. K. Maca, H. Hadraba and J. Cihlar, *Ceramics International*, 2004, **30**, 843-851
51. T. Olding, M. Sayer and D. Barrow, *Thin Solid Films*, 2001, **398-399**, 581-586
52. S. Ould-Chikh, N. Brodusch, N. Crozet, M. Hemati and L. Rouleau, *Powder Technology*, 2013, **237**, 255-265
53. W. Schwieger, M. Hartmann, T. Schwarz, H. Döring, E. Klemm and S. Schirrmeister, *Chemie Ingenieur Technik*, 2010, **82**, 921-928
54. L. Zhao, M. Bram, H. Buchkremer, D. Stover and Z. Li, *Journal of Membrane Science*, 2004, **244**, 107-115
55. C. J. Brinker, and A. J. Hurd, *J. Phys. III France,* 1994, **4**, 1231-1242
56. E. J. A. Pope, A. Almazan and K. Kratsch, *J. Am. Ceram. Soc.,* 1991, **74**, 1722-1724
57. I Santacruz, B. Ferrari, M. I. Nieto and R. Moreno, *Adv. Engineering Materials,* 2003, **5**, 647-650
58. M. Vargová, G. Plesch, U. F. Vogt, M. Zahoran, M. Gorbár and K. Jesenák, *Applied Surface Science*, 2011, **257**, 4678-4684
59. A. Maione, F. Andre and P. Ruiz, *Applied Catalysis B: Environmental*, 2007, **75**, 59-70
60. L. Giani, C. Cristiani, G. Groppi and E. Tronconi, *Applied Catalysis B: Environmental*, 2006, **62**, 121-131
61. M. Valentini, G. Groppi, C. Cristiani, M. Levi, E. Tronconi and P. Forzatti, *Catalysis Today*, 2001, **69**, 307-314
62. C. G. Visconti, E. Tronconi, L. Lietti, G. Groppi, P. Forzatti, C. Cristiani, R. Zennaro and S. Rossini, *Applied Catalysis A: General*, 2009, **370**, 93-101
63. G. Groppi, W. Ibashi, M. Valentini and P. Forzatti, *Chemical Engineering Science*, 2001, **56**, 831-839
64. P. Heinl, A. Rottmair, C. Körner and R. F. Singer, *Adv. Eng. Mater.*, 2007, **9**, 360-364
65. T. Horneber, C. Rauh and A. Delgado, *Chemical Engineering Science*, 2014, **117**, 229-238